Scattering instruments

Figure 1 shows a schematic of the small-angle neutron scattering (SANS) spectrometer LOQ at ISIS at Rutherford Laboratory in the UK. LOQ shows many features that are common to SANS and small-angle x-ray scattering (SAXS) facilities around the world, namely a collimated incident beam of probe particles, neutrons or photons, and a detector that measures the intensity of probes scattered through some angle Φ. Of course, SANS instruments are invariably located at large facilites, since the neutron beam requires a reactor or a spallation source of neutrons. There are also many SAXS facilities located at synchrotron x-ray sources, where the finest angular resolution can be achieved and the most weakly scattering samples can be studied. (BTW, many of these facilities themselves hold yearly summer (or winter or spring or fall) schools to introduce potential new users to their capabilities. More generally, access is straightforward via a short peer-reviewed proposal system.) For coarser resolution and strongly scattering samples in-house SAXS

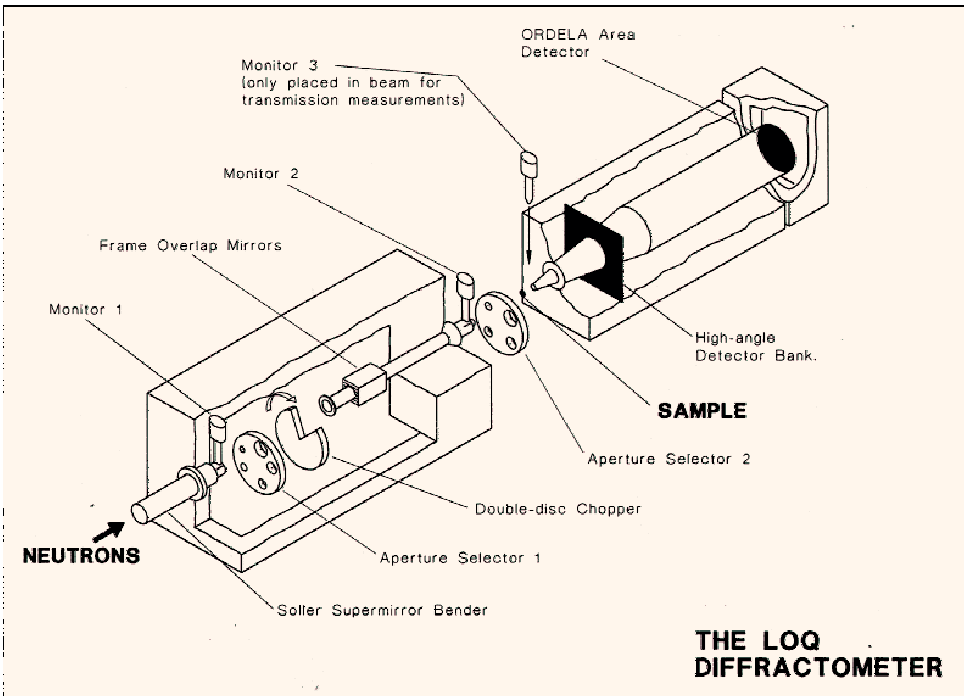

Figure 1: LOQ SANS spectrometer at ISIS (from the ISIS web site).

facilities are suitable and available. Optical light scattering setups, of course, are in-house.

In the case of LOQ, and in many cases, the detector is actually an area detector that resolves the scattering over a range of angles simultaneously. These sorts of instruments determine the scattered intensity, which in turn enables the experimenter to deduce something about the static structure of the sample. SANS and SAXS experiments are generally sensitive to structures with length scales in the range from 1 nm or less to 100 nm or more. This is just the range relevant to typical soft matter systems.

In principle, not only can the scattering angle of a given scattered probe particle be determined, but so can its energy, and in particular its energy loss to the samples. Measurements of the energy/frequency spectrum of the scattered probe particles, tell us about the sample's dynamics. Usually, however, in soft matter systems the probe particles' energy change is very small, corresponding to the low energy of dynamical modes within soft matter systems. Consequently, it is often convenient to characterize the sample's dynamics in the time domain, rather than the frequency domain. The methods used for this will be described in more detail below.

Above are a picture of the Advanced Photon Source at Argonne National Laboratory – currently, the US's brightness synchrotron – together with pictures inside the hutch at beamline 8-ID which is set up for SAXS and so-called x-ray photon correlation spectroscopy experiments.

Scattering cross-sections

Let's examine what actually happens in a scattering measurement and what is measured. In general, there is a more-or-less collimated source of incident "particles" – photons or neutrons – which impinges onto a sample of thickness W. We will suppose that the mean wavevector of the incident particles is $\mathbf{k}_i = k\hat{\mathbf{y}}$ and that their mean energy is E_i. The cross-sectional area of the incident beam (A), the number of particles incident per second (n_i), and, consequently, the incident flux ($J_i = n_i/A$) are known.

Inhomogeneities within the sample then give rise to scattering, which may be characterized by means of a detector, counting the number of particles scattered each second (n_s) into the solid angle subtended by the detector ($\Delta\Omega$). The scattering angle defined by the detector acceptance determines the wavevector of the detected particles ($\mathbf{k}_f$). A key quantity for scattering

experiments is the scattering wavevector $\mathbf{Q} = \mathbf{k}_i - \mathbf{k}_f$.

In terms of the experimental quantities (ignoring the effect of absorption), the scattering cross-section ($d\sigma/d\Omega$) and the cross-section per unit volume (Σ) are given by

$$\frac{d\sigma}{d\Omega} = \frac{n_s}{J_i \Delta\Omega} \tag{1}$$

and

$$\Sigma = \frac{n_s}{n_i W \Delta\Omega} \tag{2}$$

It is typical to present experimental measurements of the cross-section per unit volume, because that quantity is independent of the experimental configuration, depending solely on the material of the sample. Conventionally, the dimensions of Σ are inverse centimeters.

In the case that the detection scheme allows the energies of the scattered particles (E_f) to be determined to within a precision ΔE, we have

$$\frac{d^2\sigma}{d\Omega dE_f} = \frac{n_s}{J_i \Delta\Omega \Delta E}. \tag{3}$$

Inelastic neutron scattering

An important example to consider for soft matter studies is the scattering of neutrons by the nucleii within a sample. To calculate the neutron scattering cross-section, we consider a neutron within a cube of volume $V = L^3$, initially in a plane wave state $|\mathbf{k}_i >= L^{\frac{-3}{2}} e^{i\mathbf{k}_i \cdot \mathbf{r}}$. For such a state, the particle flux is simply $J_i = (v/L)/L^2$, where $v = \hbar k_i/m$ is the neutron velocity. Meanwhile, the initial state of the sample is $|\lambda_i >$. We are interested in the probability per unit time that the neutron makes a transition to a state $|\mathbf{k}_f >$, which is a plane wave state for which the wavevector lies within $\Delta\Omega$, while at the same time the sample makes a transition to state $|\lambda_f >$. Time-dependent perturbation theory (Fermi's Golden Rule) gives the general formula for the transition probability per unit time (W_{if}). Specifically,

$$W_{if} = \frac{2\pi}{\hbar} | < \mathbf{k}_i, \lambda_i | U | \mathbf{k}_f, \lambda_f > |^2 \rho(E_f), \tag{4}$$

where U is the probe-sample interaction, $\rho(E_f) = L^3 m \hbar k_f \Delta\Omega/(2\pi\hbar)^3$ is the density of final states appropriate for a particle of mass m. This is just the

value of n_s corresponding to an incident flux of $J_i = \hbar k_i / mL^3$. It follows from Eq. 1 that

$$\begin{aligned}\frac{d\sigma}{d\Omega} &= \frac{mL^3}{\hbar k_i} W_{if} \frac{1}{\Delta\Omega} \\ &= L^6 \left(\frac{m}{2\pi\hbar^2}\right)^2 \frac{k_f}{k_i} | < \mathbf{k}_i, \lambda_i | U | \mathbf{k}_f, \lambda_f > |^2. \end{aligned} \tag{5}$$

Conservation of energy is implicit in Eq. 5, so that $E_f + E_{\lambda_f} = E_i + E_{\lambda_i}$. It is convenient to make this condition explicit, so that

$$\begin{aligned}\frac{d^2\sigma}{d\Omega dE_f} &= L^6 \left(\frac{m}{2\pi\hbar^2}\right)^2 \frac{k_f}{k_i} | < \mathbf{k}_i, \lambda_i | U | \mathbf{k}_f, \lambda_f > |^2 \\ &\times \delta(\hbar\omega - E_{\lambda_f} + E_{\lambda_i}), \end{aligned} \tag{6}$$

where $\hbar\omega = E_i - E_f$ is the energy loss of the neutron, and E_{λ_f} and E_{λ_i} are the energies corresponding to $|\lambda_f >$ and $|\lambda_i >$, respectively. Ordinarily, the sample will initially be in one of many of possible initial states – with probability p_{λ_i} – and there will be a number of possible final states. Thus, the measured cross-section will be an average over initial states and a sum over final states, *i.e.*

$$\begin{aligned}\frac{d^2\sigma}{d\Omega dE_f} &= L^6 \left(\frac{m}{2\pi\hbar^2}\right)^2 \frac{k_f}{k_i} \\ &\times \sum_{\lambda_f} \sum_{\lambda_i} p_{\lambda_i} | < \mathbf{k}_i, \lambda_i | U | \mathbf{k}_f, \lambda_f > |^2 \\ &\times \delta(\hbar\omega - E_{\lambda_f} + E_{\lambda_i}), \end{aligned} \tag{7}$$

The interaction interaction potential experienced by a neutron located at $\mathbf{r}$ will be of the form

$$U = U(\mathbf{r}) = \sum_l U_l(\mathbf{r} - \mathbf{r}_l), \tag{8}$$

where $\mathbf{r}_l$ is the position of nucleus l and U_l describes its interaction with the neutron. Thus, where $\mathbf{Q} = \mathbf{k}_i - \mathbf{k}_f$ and

$$U_l(\mathbf{Q}) = \int d^3\mathbf{r} e^{i\mathbf{Q}\cdot\mathbf{r}} U_l(\mathbf{r}). \tag{9}$$

It is now convenient to write

$$\delta(\hbar\omega + E_{\lambda_i} - E_{\lambda_f}) = \frac{1}{2\pi\hbar}\int_{-\infty}^{\infty} dt e^{-i(\omega + E_{\lambda_i}/\hbar - E_{\lambda_f}/\hbar)t}, \tag{10}$$

so that

$$\begin{aligned}
\frac{d\sigma}{d\Omega dE_f} &= \left(\frac{m}{2\pi\hbar^2}\right)^2 \frac{k_f}{k_i} \\
&\times \frac{1}{2\pi\hbar}\int_{-\infty}^{\infty} dt e^{-i\omega t} \\
&\times \sum_{\lambda_f}\sum_{\lambda_i} p_{\lambda_i} < \lambda_i| \sum_l U_l(-\mathbf{Q}) e^{-i\mathbf{Q}\cdot\mathbf{r}_l} |\lambda_f > \\
&\times < \lambda_f| e^{iE_{\lambda_f}t/\hbar} \sum_m U_m(\mathbf{Q}) e^{i\mathbf{Q}\cdot\mathbf{r}_l} e^{-iE_{\lambda_i}t/\hbar} |\lambda_i > .
\end{aligned} \tag{11}$$

Using the Heisenberg representation for operators and states, we have, for example, that

$$< \lambda_f| e^{iE_{\lambda_f}t} e^{i\mathbf{Q}\cdot\mathbf{r}_m} e^{-iE_{\lambda_i}t} |\lambda_i > = < \lambda_f| e^{i\mathbf{Q}\cdot\mathbf{r}_m(t)} |\lambda_i > . \tag{12}$$

Since the $|\lambda_f >$ form a complete set of states, the sum over λ_f can be performed, and it follows that

$$\begin{aligned}
\frac{d\sigma}{d\Omega dE_f} &= \left(\frac{m}{2\pi\hbar^2}\right)^2 \frac{k_f}{k_i} \\
&\times \frac{1}{2\pi\hbar}\int_{-\infty}^{\infty} dt e^{-i\omega t} \\
&\times \sum_l \sum_m < e^{-i\mathbf{Q}\cdot\mathbf{r}_l} U_l(-\mathbf{Q}) U_m(\mathbf{Q}, t) e^{i\mathbf{Q}\cdot\mathbf{r}_m(t)} >,
\end{aligned} \tag{13}$$

where we have introduced the notation $\sum_{\lambda_i} p_{\lambda_i} < \lambda_i|...|\lambda_i > = < ... >$.

For non-magnetic materials, neutron scattering arises from the neutron-nucleus interaction. In this case, neutron scattering is sensitive to the distribution of nucleii within a sample. Theory does not (yet) predict what this interaction will be for a given nucleus. However, because the range of this interaction is so small compared to the neutron wavelength of thermal neutrons, the scattering is isotropic and may be characterized by a single quantity for each nucleus – the s-wave scattering length, usually called b –

whose value is tabulated for different nucleii and which may be positive or negative. For a nucleus of type l, the scattering length is b_l. To ensure the correct dimensions (so that b_l is a length), we must take $U_l(\mathbf{Q}) = 2\pi\hbar^2 b_l/m$. Therefore, for neutron-nuclear scattering

$$\begin{aligned}\frac{d\sigma}{d\Omega dE_f} &= \frac{k_f}{k_i} \\ &\times \frac{1}{2\pi\hbar}\int_{-\infty}^{\infty} dt e^{-i\omega t} \\ &\times \sum_l \sum_m < e^{-i\mathbf{Q}\cdot\mathbf{r}_l} b_l b_m e^{i\mathbf{Q}\cdot\mathbf{r}_m(t)} > . \end{aligned} \tag{14}$$

This expression informs us that neutron scattering is sensitive to the distribution of scattering lengths within the sample.

Even in an elemental material the scattering length can depend on position, firstly, because different isotopes have different scattering lengths, and, secondly, because states of different total angular momentum – note that the neutron has spin $\frac{1}{2}$ – have different scattering lengths. In fact, one of the most powerful aspects of neutron scattering follows from the fact that the scattering length of hydrogen is very different from the scattering length of the chemically identical deuterium.

In cases that the configurational average over isotopes and spin states is independent of the average over the nuclear coordinates – they are independent, random variables – we have

$$\begin{aligned} < b_l b_m > &= \bar{b}^2, \ \mathbf{r}m for\ l \neq m \\ &= \bar{b^2}, \ \mathbf{r}m for\ l = m, \\ &= \bar{b}^2 + \delta_{lm}(\bar{b^2} - \bar{b}^2). \end{aligned} \tag{15}$$

It follows that

$$\begin{aligned}
\frac{d\sigma}{d\Omega dE_f} &= \bar{b}^2 \frac{k_f}{k_i} \\
&\times \frac{1}{2\pi\hbar} \int_{-\infty}^{\infty} dt e^{-i\omega t} \\
&\times \sum_l \sum_m < e^{-i\mathbf{Q}\cdot\mathbf{r}_l} e^{i\mathbf{Q}\cdot\mathbf{r}_m(t)} > \\
&+ (\bar{b^2} - \bar{b}^2) \frac{k_f}{k_i} \\
&\times \frac{1}{2\pi\bar{h}} \int_{-\infty}^{\infty} dt e^{-i\omega t} \\
&\times \sum_l < e^{-i\mathbf{Q}\cdot\mathbf{r}_l} e^{i\mathbf{Q}\cdot\mathbf{r}_l(t)} > . \qquad (16)
\end{aligned}$$

The first of these terms corresponds to what is called "coherent scattering". The second term is "incoherent scattering". The double sum in the expression for coherent scattering can give rise to strong interference effects between different nucleii, leading to a strong variation of the coherent scattering cross-section versus wavevector. By contrast, the incoherent scattering, which depends on motions of the individual nucleii, varies weakly with wavevector.

The connexion between scattering and correlation functions

It is now useful to introduce the nuclear number density that is, the number of nucleii per unit volume,

$$n(\mathbf{r}, t) = \sum_l \delta(\mathbf{r} - \mathbf{r}_l(t)). \qquad (17)$$

We may introduce the Fourier transform of the number density, $n(\mathbf{Q}, t)$, via

$$n(\mathbf{Q}, t) = \int d^3\mathbf{r} n(\mathbf{r}, t) e^{-i\mathbf{Q}\cdot\mathbf{r}} = \sum_l e^{-i\mathbf{Q}\cdot\mathbf{r}_l(t)}. \qquad (18)$$

It follows that

$$< \sum_j e^{-i\mathbf{Q}\cdot\mathbf{r}_j(0)} \sum_l e^{i\mathbf{Q}\cdot\mathbf{r}_l(t)} > =< n(\mathbf{Q})n(-\mathbf{Q},t) >$$

$$= \int d^3\mathbf{r}d^3\mathbf{r}' e^{-i\mathbf{Q}\cdot(\mathbf{r}'-\mathbf{r})} < n(\mathbf{r}',0)n(\mathbf{r},t) >$$

$$= V \int d^3\mathbf{r} e^{i\mathbf{Q}\cdot\mathbf{r}} < n(\mathbf{0},0)n(\mathbf{r},t) >,$$

$$= V \int d^3\mathbf{r} e^{i\mathbf{Q}\cdot\mathbf{r}} G(\mathbf{r},t), \tag{19}$$

where V is the sample volume, and the last equality defines $G(\mathbf{r},t)$. We may use Eq. 19 to write

$$\begin{aligned}
\frac{d\sigma}{d\Omega dE_f} &= \bar{b}^2 \frac{k_f}{k_i} \\
&\times \frac{1}{2\pi\bar{h}} \int_{-\infty}^{\infty} dt e^{-i\omega t} \\
&\times V \int d^3\mathbf{r} e^{i\mathbf{Q}\cdot\mathbf{r}} G(\mathbf{r},t) \\
&+ (\bar{b^2} - \bar{b}^2) \frac{k_f}{k_i} \\
&\times \frac{1}{2\pi\bar{h}} \int_{-\infty}^{\infty} dt e^{-i\omega t} \\
&\times \sum_l < e^{-i\mathbf{Q}\cdot\mathbf{r}_l} e^{i\mathbf{Q}\cdot\mathbf{r}_l(t)} > .
\end{aligned} \tag{20}$$

This equation expresses the basic and important result that we have been aiming towards. Specifically, it is that the coherent cross-section is the product of two parts:

- A bit that depends on the interaction of neutrons with the nucleii of the sample, independent of the arrangement and motions of those nucleii: $\frac{k_f}{k_i}\bar{b}^2 N/\bar{h}$
- A bit, called the dynamic structure factor $[S(\mathbf{Q},\omega)]$ that depends on the collective properties – its structure and dynamics – of the sample:

$$S(\mathbf{Q},\omega) = \frac{1}{2\pi N} \int_{-\infty}^{\infty} dt e^{-i\omega t} < n(\mathbf{Q})n(-\mathbf{Q},t) > \tag{21}$$

$$= \frac{1}{2\pi\bar{n}} \int_{-\infty}^{\infty} dt e^{-i\omega t} \int d^3\mathbf{r} e^{i\mathbf{Q}\cdot\mathbf{r}} G(\mathbf{r}, t) \tag{22}$$

This separation, which is always found for weakly interacting probes, is one of the reasons that makes weak scattering probes so informative. *i.e.* It is not necessary to worry about disentangling the physics of the sample from the physics of the measurement.

Detailed balance and sum rules

There are a number of additional key properties of $S(Q, \omega)$.

- Detailed balance:

$$S(Q, -\omega) = e^{-\bar{h}\omega/(k_B T)} S(Q, \omega). \tag{23}$$

  This reflects the fact that in order to take energy out of the system, the system must be in a higher energy state, whose population is suppressed by a Boltzmann factor.

- The fluctuation-dissipation theorem:

$$S(Q, \omega) = \frac{2\bar{h}}{1 - e^{-\bar{h}\omega/(k_B T)}} \chi''(Q, \omega) \simeq \frac{2k_B T}{\omega} \chi''(Q, \omega), \tag{24}$$

  where the last equality holds in the classical limit. The FDT relates spontaneous thermal fluctuations, expressed via $S(Q, \omega)$, to energy loss (dissipation), expressed via the imaginary part of the dynamic susceptibility $[\chi''(Q, \omega)]$.

- The f-sum rule:

$$\int_{-\infty}^{\infty} d\omega 2\omega \chi''(Q, \omega) = \frac{Q^2}{m}. \tag{25}$$

  This is the f-sum rule for the particle density correlation function. (m is the mass of the particles in question.) Classically, this reads

$$\int_{-\infty}^{\infty} d\omega \omega^2 S(Q, \omega) = \frac{k_B T Q^2}{m}. \tag{26}$$

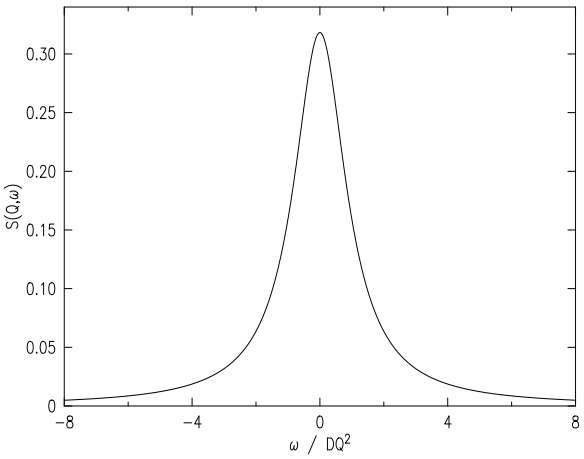

Figure 2: Dynamic structure factor for diffusion – a Lorentzian lineshape. Note the pronounced tails of the profile.

As a simple example, we calculate the coherent inelastic scattering cross-section for a system in which particle diffusion is the dominant process at long distances and times, *i.e.* small Q and ω. To carry out this program, according to Eq. 22 we need to calculate $G(\mathbf{r}, t)$, which we can do by employing Onsager's Regression Hypothesis. The Regression Hypothesis states that spontaneous fluctuations relax according to the same equations as do imposed disturbances. In the case of a dilute system of diffusing particles, an imposed disturbance $[n(\mathbf{r}, t)]$ will relax according to the diffusion equation:

$$\frac{\partial n(\mathbf{r}, t)}{\partial t} = D\nabla^2 n(\mathbf{r}, t), \tag{27}$$

where D is the diffusion coefficient. Eq. 27 is most easily solved by taking the spatial Fourier transform, so that

$$n(\mathbf{Q}, t) = e^{-DQ^2 t} n(\mathbf{Q}, 0). \tag{28}$$

The Regression Hypothesis then implies [with $n(\mathbf{Q}, 0) = n(\mathbf{Q})$] that

$$< n(\mathbf{Q}) n(\mathbf{Q}, t) >= e^{-DQ^2|t|} < |n(\mathbf{Q})|^2 > . \tag{29}$$

A basic result of statistical mechanics is that, in the limit of small wavevectors,

$$< |n(\mathbf{Q})|^2 >= N\bar{n} k_B T \chi_T, \tag{30}$$

where χ_T is the isothermal (osmotic) compressibility and $\bar{n}$ is the mean number density.

Now, we can write down the dynamic structure factor as

$$S(\mathbf{Q},\omega) == \frac{\bar{n}k_BT\chi_T}{2\pi}\frac{2DQ^2}{\omega^2+(DQ^2)^2}. \tag{31}$$

Note that or uncorrelated particles, $\chi_T = (\bar{n}k_BT)^{-1}$ from statistical mechanics.

At fixed Q, Eq. 31 corresponds to a Lorentzian function of ω. The half-width-at-half-maximum (HWHM) equals DQ^2 and the peak intensity equals $(DQ^2)^{-1}$, so that considered as a function of ω the area is independent of Q.

An interesting aspect of Eq. 31 is that it actually violates the f-sum rule (Eq. 26), because of a divergence in the sum rule integral that is the result of a too-slow decay of $S(Q,\omega)$ at large ω. Therefore, the Lorentzian lineshape cannot be the whole story. To investigate where the f-sum rule leads, let's suppose that the the Lorentzian is correct at small ω, but that at large ω there's a new microscopic time, τ, that causes $S(Q,\omega)$ to fall below the diffusion result. To account for τ, let's add an *ad hoc* additional term to the denominator that will serve to make the integral convergent:

$$S(\mathbf{Q},\omega) = \frac{\bar{n}k_BT\chi_T}{2\pi}\frac{2DQ^2}{\omega^2+\omega^4\tau^2+(DQ^2)^2}. \tag{32}$$

In this case, the f-sum rule *is* satisfied, and implies approximately (ignoring constant factors) that

$$\bar{n}k_BT\chi_T\frac{2DQ^2}{\tau} \simeq \frac{k_BTQ^2}{m} \tag{33}$$

whence

$$D \simeq \tau/(\bar{n}\chi_T m). \tag{34}$$

This is a (crude) example of a sum rule calculation.

The intermediate scattering function (ISF)

It is rather straightforward to conceive of how an inelastic scattering measurement might be carried out. Such measurements require the source of radiation to have a well-defined energy and the detection scheme to be able

to resolve energy. Bragg reflection from crystals is one way to perform the monochromatization needed. However, it is difficult to resolve very small energy changes. Therefore, to study low-energy, *i.e.* slow, processes – which, typically, are of principal interest in soft matter systems – techniques have been devised that instead of directly determining the dynamic structure factor $[S(Q,\omega)]$ yield the inverse Fourier transform of the dynamic structure factor, namely the intermediate scattering function (ISF):

$$S(Q,t) = \int_{-\infty}^{\infty} d\omega e^{i\omega t} S(Q,\omega). \tag{35}$$

For example, in the case of diffusion, by substituting Eq. 31 into Eq. 35 we find

$$S(Q,t) = \bar{n} k_B T \chi_T e^{-DQ^2 t}, \tag{36}$$

corresponding to a simple exponential decay of the ISF versus t.

Static structure factor

In fact, in many (even most) cases, scattering experiments do not energy resolve the scattered radiation. Instead, scattered radiation of all frequencies is accepted by the detector and what is measured is then the integral of $S(Q,\omega)$ over frequency:

$$\frac{d\sigma}{d\Omega} = N\bar{b}^2 \int_{-\infty}^{\infty} d\omega \frac{k_f}{k_i} S(Q,\omega). \tag{37}$$

In many cases, it is also an excellent approximation that $k_f \simeq k_i$, whence

$$\frac{d\sigma}{d\Omega} = N\bar{b}^2 \int_{-\infty}^{\infty} d\omega S(Q,\omega) = N\bar{b}^2 S(Q,0), \tag{38}$$

where $S(Q,0) = S(Q)$ is the ISF evaluated at $t = 0$. $S(Q)$ is generally called the static structure factor. It is imperative to understand that a measurement of $S(Q)$ corresponds to a $t = 0$ correlation function, *i.e.* a measure of the instantaneous correlations – a snapshot.

How exactly is $S(Q)$ related to correlation functions? The answer is that

$$S(Q) = \sum_l \sum_m < e^{-i\mathbf{Q}\cdot\mathbf{r_l}} e^{i\mathbf{Q}\cdot\mathbf{r_m}} >= V \int d^3\mathbf{r} e^{i\mathbf{Q}\cdot\mathbf{r}} G(\mathbf{r},0). \tag{39}$$

That is, $S(Q)$ is the space Fourier transform of $G(r,0)$.

For an ideal gas, the particles are uncorrelated with each other. It follows that $G(r,0) =< n(\mathbf{r})n(\mathbf{0}) >=< n(\mathbf{r}) >< n(\mathbf{0}) >= \bar{n}^2$. It is conventional to introduce the pair correlation function, $g(r) = G(r,0)/\bar{n}^2$, often also called the radial distribution function (in the case of an isotropic system) or the pair distribution function. For an ideal gas, $g(r) = 1$. We can get further insight into the pair correlation function by noting that the number of particles in a volume ΔV at the origin is $n(\mathbf{0})\Delta V$. It follows that the probability of there being a particle in ΔV at the origin is $< n(0) > \Delta V/N = \bar{n}\Delta V/N$, where N is the total number of particles in the system. Similarly, the probability of there being a particle in ΔV at the origin and in ΔV at position $\mathbf{r}$ is $(\Delta V)^2 < n(\mathbf{r})n(\mathbf{0})n(\mathbf{r}) > /N^2$. A theorem of probability theory now informs us that the ratio of these probabilities, i.e. $(\Delta V/N) < n(\mathbf{r})(n(\mathbf{0}) > /\bar{n} = (\Delta V/N)\bar{n}g(r)$, is the conditional probability that a particle will be found in ΔV at $\mathbf{r}$, given that a particle is at the origin. Alternatively, $\bar{n}g(r)$ is the mean density of particles at $\mathbf{r}$, given that a particle is at the origin.

Neutron spin echo

The method employed to measure the ISF using neutrons is the neutron spin echo (NSE) technique [Mezei(1972)], which is capable of probing times between about 10^{-9} and 2×10^{-7} second. NSE uses the precession of the neutron spin in a transverse magnetic field in order to probe changes in the neutron velocity and thus energy. Conceptually, a NSE experiment is carried out as follows. A beam of neutrons is polarized initially parallel to the neutron momentum. Then a $\pi/2$ flipper is used to change the polarization to be perpendicular to the neutron momentum and then passes through a region where there is a magnetic field whose direction is transverse to the neutron polarization, and parallel to the neutron's momentum. Thus, each neutron spin precesses through an angle that depends on the time the neutron spends in the magnetic field region, hence on the neutron velocity and energy. Typically, neutrons perform several thousand precessions. Then, the neutron beam scatters from the sample. Any neutron that is to be detected preserves its spin in the scattering process, so that NSE probes coherent scattering. Immediately after scattering at the sample position, the neutron passes through a π flipper, so that in the same magnetic field, it will precess in the opposite sense. Next, indeed the scattered neutron does pass into an-

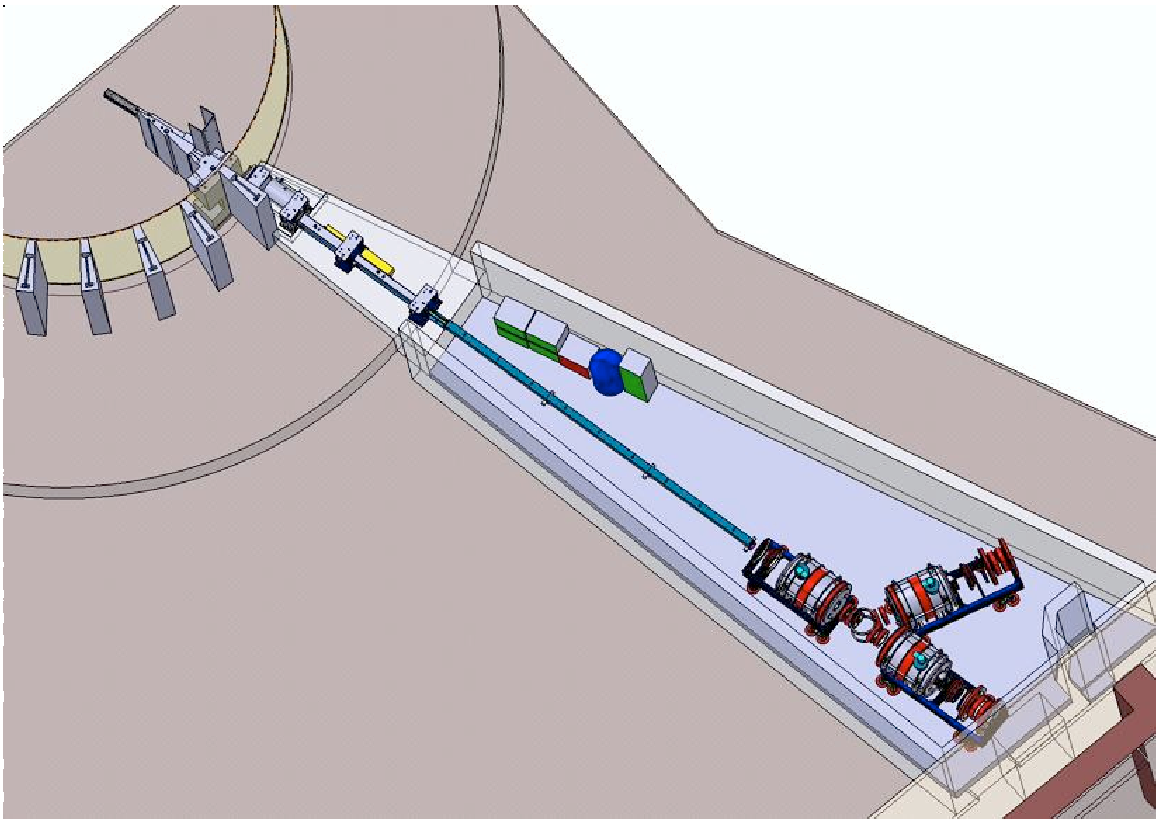

Figure 3: A schematic drawing of the neutron spin echo spectrometer installed at beamline 15 at the Spallation Neutron Source.

other region where the magnetic field is equal to that in the first precession region. For elastically scattered neutrons, the effect of this second precession region, which is supposed to be of precisely the same length as the first, is to undo the original precession, so that elastically scattered neutrons exit this region with a well-defined polarization. Next, there is another $\pi/2$ flipper to prepare the beam for polarization analysis. The final polarization analysis of the neutron beam yields unity for elastically scattered neutrons. By contrast, inelastically scattered neutrons have either precessed too far (for neutrons that have lost energy) or too little (for neutrons that have gained energy) for the initial precession to be exactly undone. This is by virtue of the longer or shorter time, respectively, spend in the second precession region. Consequently, polarization analysis of inelastically scattered neutrons generally yields an average that is less than unity. Specifically, for a given change in the neutron energy of $\hbar\omega$, the corresponding neutron polarization may be shown to be $P(\omega) \simeq \cos(2\pi N_0 \hbar\omega/E)$, where N_0 is the number of precessions made in the first precession region, and E is the mean neutron energy. On the other hand, the fraction of the neutrons suffering an energy change of $\hbar\omega$ is $S(Q,\omega)/S(Q)$, where $S(Q) = \int_{-\infty}^{\infty} d\omega S(Q,\omega)$. Thus, for a given setting of N_0, the polarization of the neutron beam is

$$\bar{P} = \frac{\int_{-\infty}^{\infty} d\omega P(\omega) S(Q,\omega)}{S(Q)} = \frac{\int_{-\infty}^{\infty} d\omega S(Q,\omega) \cos(2\pi N_0 \hbar\omega/E)}{S(Q)} = \frac{S(Q, 2\pi N_0 \hbar/E)}{S(Q)}, \tag{40}$$

which is just the normalized intermediate scattering function for a "time" $2\pi N_0 \hbar/E$. It is therefore possible to measure $S(Q,t)/S(Q)$ versus t by measuring the polarization at different magnetic field strengths, because N_0 depends on magnetic field.

Picturesquely, we may say that the neutron spin is like the hand of an internal clock attached to each individual neutron, which may be used to measure the difference in time spent in the two precession regions, and hence the change in the neutron energy upon scattering.

Notice that to achieve long times, or equivalently small energy transfers, N_0 should be as large as possible. There are important requirements on the uniformity and extent of the magnetic fields which limit the longest times achievable.

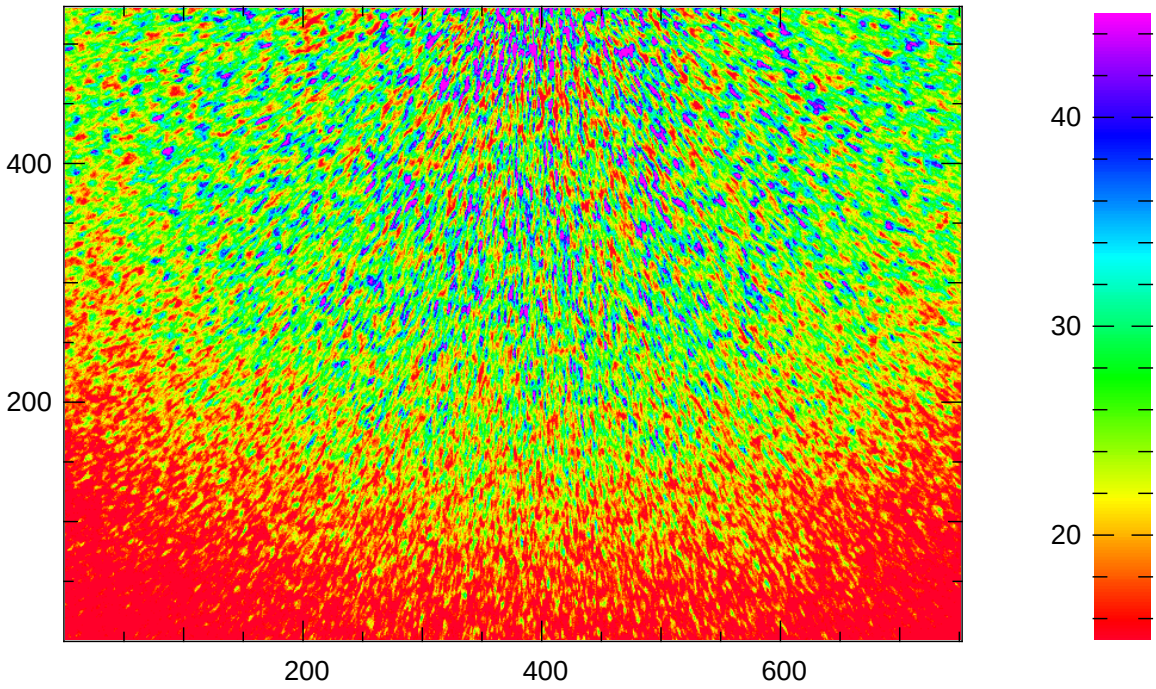

Figure 4: Aerogel speckle pattern, obtained with a partially coherent x-ray beam.

Photon correlation spectroscopy

The method alternately known as photon correlation spectroscopy (PCS), quasielastic light scattering (QELS), intensity fluctuation spectroscopy (IFS), or dynamic light scattering (DLS) also measures $S(Q,t)$. Key to performing PCS measurements is a partially coherent beam. What is a coherent beam? Crudely, we can say that in a partially coherent beam the value of the electric field at a given point in the sample is correlated with the value at another, distant point in the sample. If such a beam is used in a scattering experiment, fluctuations in the scattered intensity arise as a result of interference among the fields scattered by different particles. This is speckle. Fig. 4 illustrates a CCD image of x-ray speckle from a completely static sample – a piece of aerogel. The implementation of PCS requires a certain coherence of the incident light and detection scheme, that is not required for inelastic scattering techniques, nor for NSE. Useful coherence, however, requires brightness, which precludes the use of neutrons.

PCS with laser light has long been employed to investigate the dynamics of condensed matter on micrometer length scales and time scales from submicroseconds to hundreds of seconds or longer [Chu(1974)]. More recently, with very bright synchrotron sources, it has become possible to carry out PCS experiments with x-rays on time scales of milliseconds, or less, under special circumstances. (X-ray PCS is one of the things I do, so my examples will often involve x-rays.) In either case, the speckle pattern varies in time as the sample undergoes thermal fluctuations, so that the time variations of the speckle pattern directly mirror the time variations of density/refractive index fluctuations within the sample. Here is x-ray speckle from a dynamic sample of 190-nm-radius colloidal particles suspended in water.

The determine the characteristic relaxation rates of the sample, therefore, is it necessary to characterize the time variations of the speckle intensity. This may be done by determining the time autocorrelation of the intensity (g_2) in a speckle as it fluctuates on and off. For the multispeckle data shown in the movie above, we calculate g_2 pixel-by-pixel and then average together all g_2 with the same Q (within some chosen resolution). The results are shown in Fig. 5, which indeed shows autocorrelation functions obtained at several representative Qs for 190 nm-radius silica spheres suspended in water. The resultant time autocorrelation function of the intensity scattered with wavevector Q $[g_2(Q,t)]$ is related to the dynamic structure factor $[S(Q,t)]$ of the sample via

$$g_2(t) = 1 + \beta[f(Q,t)]^2, \tag{41}$$

where β is the speckle contrast, and $f(Q,t) = S(Q,t)/S(Q,0)$ is the normalized intermediate scattering function.

Consider a scattering experiment in which a highly-collimated photon beam with mean wavevector $\mathbf{k}_i = k\hat{\mathbf{y}}$ is incident on a sample, for which the local electron density is $\rho(\mathbf{r},t)$, at location $\mathbf{r}$ and time t. The corresponding incident electric field at $\mathbf{r}$ and t may be written $\mathbf{E}_{inc}(\mathbf{r},t) = E_i(\mathbf{r},t)\hat{\mathbf{e}}_i e^{i(\mathbf{k}_i.\mathbf{r}-\bar{\omega})t}$, where $\bar{\omega} = \omega_i = ck$ is the mean frequency, $\hat{\mathbf{e}}_i$ is the polarization of the incident photons and c is the speed of light. We suppose that E_i is a complex amplitude that varies slowly in time compared to $2\pi/\bar{\omega}$ and slowly in space compared to $2\pi/k$. With the further assumption that the the electron density at any point varies slowly compared to $2\pi/\bar{\omega}$, the electric field at a distance R from the sample, scattered to wavevector $\mathbf{k}_f$, is

$$\mathbf{E}_f(t') = \hat{\mathbf{e}}_f \frac{\hat{\mathbf{e}}_f \cdot \hat{\mathbf{e}}_i r_0 e^{i\bar{\omega}t}}{4\pi R} \int_V d^3\mathbf{r} e^{i\mathbf{Q}\cdot\mathbf{r}} \rho(\mathbf{r},t) E_i(\mathbf{r}, t + \frac{\mathbf{k}_f.\mathbf{r}}{\bar{\omega}}), \tag{42}$$

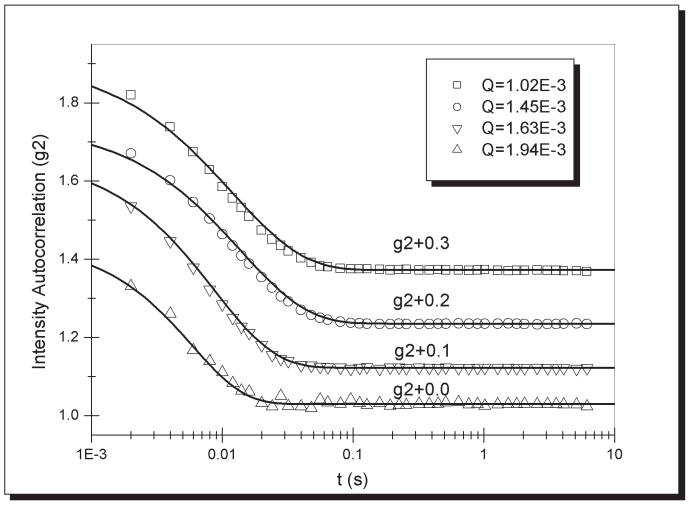

Figure 5: Intensity autocorrelation functions vs. time for 190-nm-radius silica spheres in water at the wavevectors indicated. For clarity, different g_2s have been shifted from each other.

where $\hat{\mathbf{e}}_f$ is the polarization of the scattered photon, $\mathbf{Q} = \mathbf{k}_i - \mathbf{k}_f$ is the wavevector transfer, $t' = t + R/c$ is the time at which x-rays scattered at time t are detected, and r_0 is the Thomson radius of the electron. (In fact, this expression is appropriate for x-rays. For light, it should be replaced by an expression that involves the refractive index density, rather than the charge density.) The integration volume (V) in Eq. 42 is the illuminated sample volume, which we will take to be a right-angled parallelopiped of dimensions L along x, M along z, and W along y. Since the incident field is a plane wave to a good approximation, E_i only depends on y and t in the combination $y - ct$. It follows that $E_i(x, y, z, t) = E_i(x, 0, z, t - y/c)$, so that

$$\mathbf{E}_f(t') = \hat{\mathbf{e}}_f \frac{\hat{\mathbf{e}}_f \cdot \hat{\mathbf{e}}_i r_0 e^{i\bar{\omega}t}}{4\pi R} \int_V d^3\mathbf{r} e^{i\mathbf{Q}\cdot\mathbf{r}} \rho(\mathbf{r}, t) E_i(x, 0, z, t - \frac{\mathbf{Q}.\mathbf{r}}{\bar{\omega}}), \qquad (43)$$

Using the fact that E_i and ρ are translationally invariant, independent

random variables, the corresponding mean scattered intensity is

$$< |E_f|^2 > = (\frac{\hat{\mathbf{e}}_f \cdot \hat{\mathbf{e}}_i)^2 r_0^2 V}{4\pi R^2} \int_V d^3\mathbf{r} e^{i\mathbf{Q}\cdot\mathbf{r}} \times < \rho(\mathbf{0},0)\rho(\mathbf{r},0) >< E_i(0,0,0,0)E_i^*(x,0,z,-\frac{\mathbf{Q}\cdot\mathbf{r}}{\bar{\omega}}) > . \quad (44)$$

Typically, the correlation length of fluctuations in the charge density within the sample is much shorter than the coherence lengths of the electric field.

Therefore, Eq. 44 can be written

$$< |E_f|^2 > = \frac{(\hat{\mathbf{e}}_f.\hat{\mathbf{e}}_i)^2 r_0^2 V}{4\pi R^2} < |E_i|^2 > \times \int_V d^3\mathbf{r} e^{i\mathbf{Q}\cdot\mathbf{r}} < \rho(\mathbf{0},0)\rho(\mathbf{r},0) > . \quad (45)$$

The scattering cross-section per unit volume ($\Sigma = \Sigma(\mathbf{Q})$) is defined, analogously to that for neutrons, in terms of the rate of incident x-rays (n_i) and the rate of x-rays scattered into a solid angle $\Delta\Omega$ (n_s) via

$$\frac{n_s}{n_i} = \frac{< |E_f|^2 > R^2 \Delta\Omega}{< |E_i|^2 > A} = \Sigma W \Delta\Omega, \quad (46)$$

where A is the cross-sectional area of the incident beam and W is the sample thickness along the beam. Comparison of Eq. 45 and Eq. 46 yields the result

$$\Sigma = (\hat{\mathbf{e}}_f \cdot \hat{\mathbf{e}}_i)^2 r_0^2 \int_V d^3\mathbf{r} e^{i\mathbf{Q}\cdot\mathbf{r}} < \rho(\mathbf{0},0)\rho(\mathbf{r},0) > . \quad (47)$$

The more-general formula, that also applies to optical scattering experiments, is

$$\Sigma = \frac{(\hat{\mathbf{e}}_f \cdot \hat{\mathbf{e}}_i)^2 k^4}{16\pi^2} \int_V d^3\mathbf{r} e^{i\mathbf{Q}\cdot\mathbf{r}} < \epsilon(\mathbf{0},0)\epsilon(\mathbf{r},0) >, \quad (48)$$

where $\epsilon(\mathbf{r},t)$ is the dielectric constant density at $\mathbf{r}$ and t.

The quantity measured in PCS experiments is the normalized intensity autocorrelation function, averaged over the accumulation time (T) and the detector area (A):

$$g_2(t,T,A) = \frac{1}{A^2T^2} \int_{-T/2}^{T/2} dt_1 \int_{t-T/2}^{t+T/2} dt_2 \int_A d\mathbf{s}_1^2 \int_A d\mathbf{s}_2^2 \; g_2(\mathbf{s}_1 - \mathbf{s}_2, t_1 - t_2) \quad (49)$$

where

$$g_2(\mathbf{s}_1-\mathbf{s}_2,t_1-t_2)=\frac{<|E_f(t_1)|^2|E_f(t_2)|^2>}{<|E_f|^2>^2}, \tag{50}$$

and $\mathbf{s}_1$ and $\mathbf{s}_2$ are deviations from an origin defined on the acceptance area of the detector [Jakeman(1973), Pusey(1976)]. We start by substituting Eq. 43 into Eq. 50, which yields the result that

$$\begin{aligned}
&g_2(\mathbf{s}_1-\mathbf{s}_2,t)= \\
&\quad\frac{(\hat{\mathbf{e}}_f\cdot\hat{\mathbf{e}}_x)^4r_0^4}{4\pi R^4<|E_f|^2>^2}\int_V d^3\mathbf{r}_1\int_V d^3\mathbf{r}_2\int_V d^3\mathbf{r}_3\int_V d^3\mathbf{r}_4 \\
&\quad e^{-i(\mathbf{Q}+\mathbf{s}_1)\cdot(\mathbf{r}_1-\mathbf{r}_2)}e^{-i(\mathbf{Q}+\mathbf{s}_2)\cdot(\mathbf{r}_3-\mathbf{r}_4)} \\
&\quad<\rho(\mathbf{r}_1,0)\rho(\mathbf{r}_2,0)\rho(\mathbf{r}_3,t)\rho(\mathbf{r}_4,t)> \\
&\quad<E_i(x_1,0,z_1,i-\frac{(\mathbf{Q}+\mathbf{s}_1)\cdot\mathbf{r}_1}{\bar{\omega}})E_i^*(x_2,0,z_2,-\frac{(\mathbf{Q}+\mathbf{s}_2)\cdot\mathbf{r}_2}{\bar{\omega}}) \\
&\quad E_i(x_3,0,z_3,t-\frac{(\mathbf{Q}+\mathbf{s}_1)\cdot\mathbf{r}_3}{\bar{\omega}})E_i^*(x_4,0,z_4,t-\frac{(\mathbf{Q}+\mathbf{s}_2)\cdot\mathbf{r}_4}{\bar{\omega}})>.
\end{aligned} \tag{51}$$

Significant contributions to the integrals of Eq. 51 occur for $\mathbf{r}_1\simeq\mathbf{r}_2$ and $\mathbf{r}_3\simeq\mathbf{r}_4$ and for $\mathbf{r}_1\simeq\mathbf{r}_4$ and $\mathbf{r}_2\simeq\mathbf{r}_3$, so that, in the realistic case that the coherence time of the source is much shorter than the correlation time of the sample, we find

$$\begin{aligned}
&g_2(\mathbf{s}_1-\mathbf{s}_2,t)=1+\frac{(\hat{\mathbf{e}}_f\cdot\hat{\mathbf{e}}_x)^4r_0^4}{4\pi R^4<|E_f|^2>^2} \\
&\quad\int_V d^3\mathbf{r}_1\int_V d^3\mathbf{r}_2\int_V d^3\mathbf{r}_3\int_V d^3\mathbf{r}_4 e^{i\mathbf{Q}\cdot(\mathbf{r}_1-\mathbf{r}_4)}e^{-i\mathbf{Q}\cdot(\mathbf{r}_2-\mathbf{r}_3)} \\
&\quad<\rho(\mathbf{r}_1,0)\rho(\mathbf{r}_4,t)><\rho(\mathbf{r}_2,0)\rho(\mathbf{r}_3,t)>e^{-i(\mathbf{s}_1-\mathbf{s}_2)\cdot(\mathbf{r}_1-\mathbf{r}_2)} \\
&\quad<E_i(x_1,0,z_1,-\frac{(\mathbf{Q}+\mathbf{s}_1)\cdot\mathbf{r}_1}{\bar{\omega}})E_i^*(x_2,0,z_2,-\frac{(\mathbf{Q}+\mathbf{s}_2)\cdot\mathbf{r}_2}{\bar{\omega}})> \\
&\quad<E_i(x_2,0,z_2,t+\frac{(\mathbf{Q}+\mathbf{s}_1)\cdot\mathbf{r}_2}{\bar{\omega}})E_i^*(x_1,0,z_1,t+\frac{(\mathbf{Q}+\mathbf{s}_2)\cdot\mathbf{r}_1}{\bar{\omega}})> \\
&\quad=1+\gamma(\mathbf{s}_1-\mathbf{s}_2)\left|\frac{S(Q,t)}{S(Q)}\right|^2,
\end{aligned} \tag{52}$$

where

$$S(Q,t)=\frac{V}{N}\int_V d^3\mathbf{r}e^{i\mathbf{Q}\cdot\mathbf{r}}<\rho(\mathbf{0},0)\rho(\mathbf{r},t)>, \tag{53}$$

and

$$\gamma(\mathbf{s}_1 - \mathbf{s}_2) = \int_V d^3\mathbf{r}_1 \int_V d^3\mathbf{r}_2 e^{-i(\mathbf{s}_1-\mathbf{s}_2).(\mathbf{r}_1-\mathbf{r}_2)} \times \frac{|< E_i(0,0,0,0)E_i^*(x_2-x_1,0,z_2-z_1,\mathbf{Q}.(\mathbf{r}_2-\mathbf{r}_1)/\bar{\omega})>|^2}{V^2 < |E_i|^2 >^2} \tag{54}$$

Eq. 52 demonstrates the relationship between the experimentally measured intensity autocorrelation function, on the one hand, and the ISF on the other. Carrying out the integrals over $\mathbf{s}_1$ and $\mathbf{s}_2$ yields

$$g_2(t, A) = 1 + \beta \left| f(Q, t) \right|^2, \tag{55}$$

where β depends on the source and the experimental set-up, in a fashion that is in principle understood,

In addition to averaging over the area of detector, experimentally we average over the accumulation time, T. Except in the special case of a simple exponential, temporal averaging gives rise to distortion of the ISF for large enough ΓT, as is shown by Jakeman [Jakeman(1973)]. Therefore, it is highly desirable to ensure that the product characteristic decay rate of the sample (Γ) and the accumulation time (T) is small. In this case, the quantity measured by PCS is

$$g_2(t, T, A) = 1 + \beta \left| f(Q, t) \right|^2, \tag{56}$$

and $f(Q, t)$ is the normalized ISF of the sample under study.

Exercise: A sample is illuminated by an electric field $E_i = E_0 \cos \bar{\omega} t$. Suppose that the corresponding electric field scattered from a sample into a detector is $E_f = E' \cos \omega t + E'' \sin \omega t$. E' and E'' are independent random variables, both with a Gaussian probability density with zero mean and with variance σ^2. Calculate the probability density of the intensity, defined as $I = (E')^2 + (E'')^2$?

Coil-globule transition in a single polymer chain

Now you know how the intermediate scattering function (IFS), $S(Q, t)$, can be measured. we also derived the form of $S(Q, t)$ for objects whose dynamics

follow the diffusion equation. A dilute suspension of particles in a fluid is an example. For such a system

$$S(Q,t) = N\bar{n}k_BT\chi_T e^{-DQ^2t}, \tag{57}$$

so that the IFS decays versus time with a time constant $(DQ^2)^{-1}$. Evidently, therefore, measurements of $S(Q,t)$ may be used to determine the diffusion coefficient D of the consituents of the suspension.

An elegant experiment to characterize the collapse of individual polymers as the solvent goes from good to bad was carried out by Nishio *et al.* [Nishio et al.(1979)Nishio, Sun, Swislow, and Tanaka] by using photon correlation spectroscopy (PCS) to measure the polymer diffusion coefficient. The Stokes-Einstein relation relates the diffusion coefficient (D) of a particle in a viscous medium with its hydrodynamic radius (R_H), via $D = k_BT/6\pi\eta R_H$. (The solution viscosity is η.) Thus, PCS measurements can be used to determine R_H. Fig. 6 shows Nishio *et al.*'s measurements of the hydrodynamic radius (open circles) of polyacrylamide polymers in dilute solution in water-acetone as a function of the acetone concentration. Evidently, at about 40 percent acetone by volume, the polymer radius drops sharply from about 48 nm to about 20 nm. This is termed the coil-globule transition. A computer-generate rendition of the corresponding polymer conformations are shown in Fig. 7.

A simple theory (see below), based upon minimizing the free energy of an individual polymer, explains this behavior [Grosberg and Khokhlov(1997)]. Consider a polymer composed of N monomers, each of length ℓ, so that if the polymer's conformation were that of a random walk, its r.m.s. radius would be $R \simeq N^{\frac{1}{2}}\ell$. (In this discussion, we will not be concerned with precise numerical coefficients – actually $R = (N/6)^{\frac{1}{2}}\ell$ for a random walk in three-dimensional space with step size ℓ – rather we will get the correct functional dependences on parameters of interest.)

In general, the polymer experiences interactions which tend to expand or shrink the polymer compared to a random walk to a radius αR. We may determine the effect of the interactions as follows. First, we write down the energy of a chain as

$$U(\alpha) \simeq Vk_BT(b_2n^2 + b_3n^3 + ...) \simeq k_BT(\frac{b_2N^{\frac{1}{2}}}{\alpha^3\ell^3} + \frac{b_3}{\alpha^6\ell^6}], \tag{58}$$

where, b_2 and b_3 are the second and third virial coefficients, respectively, characterizing the monomer-monomer interactions, $V \simeq \alpha^3R^3$ is the volume

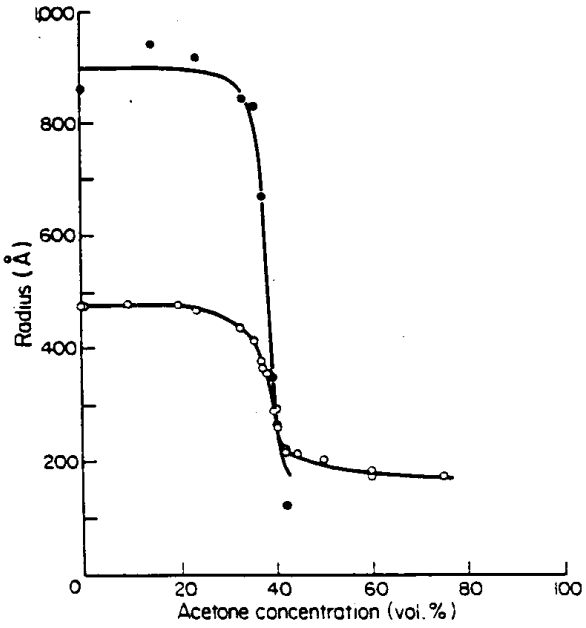

Figure 6: Hydrodynamic radius (open circles) and radius of gyration (solid circles) of polyacrylamide in water-acetone vs. acetone concentration.

Figure 7: Conformation of (a) a compact polymer globule and of (b) a polymer coil. From Ref. [Grosberg and Khokhlov(1997)].

of the coil and $n \simeq N/(\alpha R)^3$ is the number density of monomers within the polymer.

Irrespective of b_2, b_3 is positive corresponding to a hard core that prevents complete collapse of the polymer. In a good solvent, we expect b_2 to be positive, corresponding to excluded-volume interactions. In this case, $U(\alpha)$ decreases monotonically with increasing α, favoring an expanded polymer. However, in a poor solvent, the momomers are attracted to each other, so that b_2 is negative anf $U(\alpha)$ exhibits a minimum at some non-zero α.

In addition to the energy, the polymer's entropy is the second key ingredient for determining the minimum free-energy state of the polymer via $F = U - TS$ The entropy of a stretched or squeezed chain is reduced compared to that of a random walk. Specifically, it is possible to show that the entropy as a function of α is approximately

$$S(\alpha) \simeq S(0) - k_B(\alpha^2 + \frac{1}{\alpha^2} - 2). \tag{59}$$

The equilibrium conformation is then found by minimizing the free energy

$$F(\alpha) = U(\alpha) - TS(\alpha) \simeq k_B T(\frac{b_2 N^{\frac{1}{2}}}{\alpha^3 \ell^3} + \frac{b_3}{\alpha^6 \ell^6}) + k_B T(\alpha^2 + \frac{1}{\alpha^2} - 2) - TS(0). \tag{60}$$

This function is shown in Fig. 8 for several values of b_2 with b_3 fixed. Evidently, for the least negative value of b_2, $F(\alpha)$ has a minimum for $\alpha > 1$ only. For more negative values of b_2, however, a second minimum appears for $\alpha < 1$. At sufficiently negative values of b_2, the second minimum becomes the lower in free energy, and a transition between an expanded coil and a collapsed globule occurs. Thus, this simple (qualitative) theory mimics the behavior seen experimentally by Nishio et al. via their measurements of $S(Q, t)$.

Exercise: In the case that the polymer is swollen, calculate how α depends on N, and hence how R depends on N.

Static scattering from dilute spheres

We will consider the static scattering from several different objects. The first is perhaps the simplest, namely a sphere of uniform scattering length

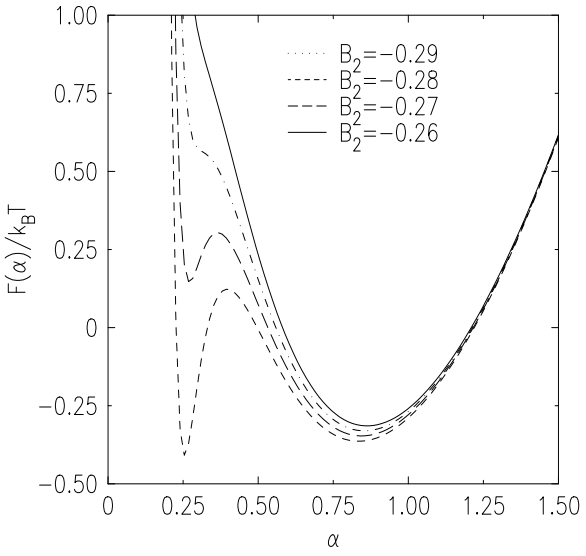

Figure 8: The free energy, $F(\alpha)/k_BT$, of a polymer as a function of its expansion, α, relative to a Gaussian coil for several values of $B_2 = b_2 N^{\frac{1}{2}}/\ell^3$ and $B_3 = b_3/\ell^6 = 0.001$.